New Results in NPID Control: Tracking, Integral Control, Friction Compensation and Experimental Results

Brian Armstrong[†], David Neevel, Todd Kusik
Department of Electrical Engineering and Computer Science, UW-Milwaukee

P.O. Box 784, Milwaukee, Wisconsin 53201

[†]bsra@uwm.edu

Keywords: Nonlinear control, Nonlinear feedback, Linear systems, Lyapunov stability, Integral control, Friction compensation

Abstract

Nonlinear (NPID) control is implemented by varying the controller gains as a function of system state. NPID control has been previously described and implemented, and recently a constructive Lyapunov stability proof has been given. Here, NPID control analysis and design methods are extended to tracking, and to systems with state feedback and integral control. Experimental results are presented showing improved tracking accuracy and friction compensation by NPID control.

1 Introduction

Nonlinear Proportional-Integral-Derivative control (NPID control) may be any control structure of the form:

$$u(t) = k_p(\cdot)\, e(t) + k_d(\cdot)\, \dot{e}(t) + k_i(\cdot) \int e(\tau)\, d\tau \tag{1}$$

where $k_p(\cdot)$, $k_d(\cdot)$ and $k_i(\cdot)$ are time-varying controller gains, and $u(t)$ and $e(t)$ are the system input and error, respectively. NPID control has a long history [1, 2, 3, 4, 5, 6, 7, 8, 9, 10] and has found two broad classes of application: i) nonlinear systems, where NPID control is used to accommodate the nonlinearity, often to achieve consistent response across a range of conditions, e.g., [4, 5, 6]; and ii) linear systems, where NPID control is used to achieve performance not achievable by linear compensation [1, 2, 3, 8, 10, 11, 12].

Here we are interested in NPID control applied to linear systems with the objective of improved performance. Past and recent studies [1, 2, 3, 6, 7, 12, 13] have shown that for linear systems NPID control can provide:

1. Increased damping,
2. Reduced rise time for step or rapid inputs,
3. Improved tracking accuracy, and
4. Friction Compensation.

Experimental demonstrations of NPID control include the Orbital Special-Purpose Dextrous Manipulator [9, 13], and the Sarcos Dextrous Manipulator [11, 14].

For linear systems, two broad categories of NPID control are found: those with gains modulated according to the magnitude of the state, and those with gains modulated according to the phase. Shahruz and Schwartz [6, 7] provide an example of magnitude-based Nonlinear Proportional-Integral control. They propose the control law:

$$\begin{aligned} \dot{\xi}(t) &= \frac{e(t)}{1+\mu^2 e^2(t)},\ \xi(0)=0 \\ u(t) &= k_i\,\xi(t) + [k_p + g_p\, e^{\lambda|e(t)|}]\, e(t) \end{aligned} \tag{2}$$

By choice of μ the integral control term can be made softer for large errors; and by choice of g_p and λ the proportional term can be made stiffer. The result is rapid transits with improved damping. The authors present an optimization technique for selecting μ, g_p and λ .

In the present study we are concerned with phase-based modulation of controller gains. This form was first proposed for the MIT/Utah hand by Jacobsen *et al.* [2]; and has been experimentally demonstrated by Xu, Hollerbach and Ma [11, 14] and others [15, 16], and theoretically justified in [1]. A simple form of phase-based NPID control is given by:

$$k_p(t) = \begin{cases} k_0 & \operatorname{sgn}(e) \neq \operatorname{sgn}(\dot{e}) \\ k_0 + k_1 & \operatorname{sgn}(e) = \operatorname{sgn}(\dot{e}) \end{cases} \tag{3}$$

Intuitively, low gain, $k_p(t) = k_0$, is applied when moving toward the goal, and high gain, $k_p(t) = k_0 + k_1$, is applied when moving away from the goal. The NPID control of Eqn (3), illustrated in figure 1, approximates the control demonstrated by Xu *et al.* [11].

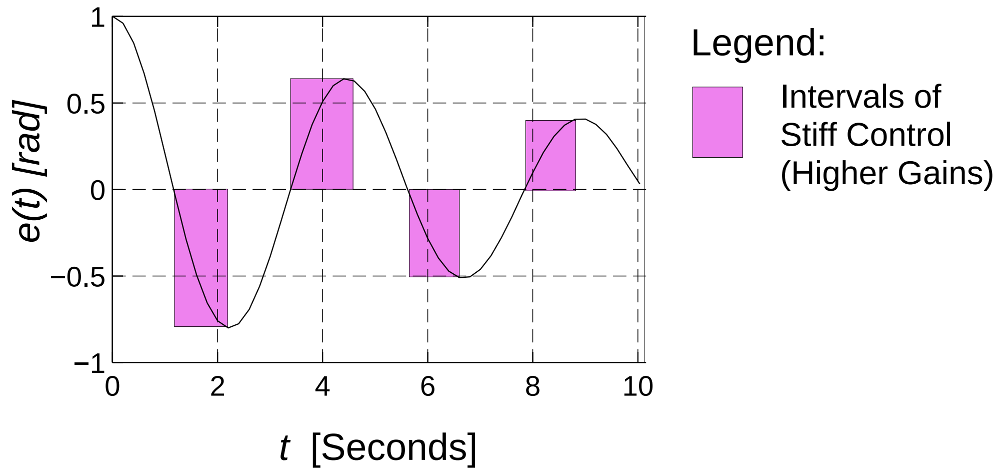

Figure 1: Illustration of NPID switching according to Eqn (3) (adapted from 3).

The improved damping of NPID control can be qualitatively understood in this way: the higher control gain, $k_p(t) = k_0 + k_1$, acts as a stiff spring while the system is moving away from the goal; the lower gain, $k_p(t) = k_0$, acts as a soft spring while moving toward the goal. With each half cycle, the stiff spring is compressed, the soft spring is relaxed, and more energy is removed from the system than is supplied.

It is clear that reversing the order of the actions, compressing the soft spring and relaxing the stiff spring, will introduce energy and reduce damping. Thus, this construction of NPID control depends on modulating control gain according to system phase. Reduced rise time is achieved by modulating the rate gain. The NPID benefits of improved tracking and friction compensation arise with the stiffness achievable when $k_p(t) = k_0 + k_1$; this high gain may be much greater than that supportable by conventional linear control [1, 12].

Control which fits within the framework of Eqn (1) has been cast as PI, PD or PID control (e.g., [7, 9, 11]) and also in state space form [1, 3, 12]; and has been called NPI, NPD and NPID control. The present results apply to any of the PI, PD or PID constructions; for simplicity, we use the term NPID control throughout this paper. The analysis and design methods to be presented are developed with a state space model, but with suitable construction of the state vector and restriction on the feedback matrices, the state space model can represent any of the PD, PI or PID combinations. For the experimental results of section 6, control is designed in state space form and implemented in the PID control form of Eqn (1).

Extension of the established results to state feedback, tracking and integral control, and experimental demonstration of improved tracking accuracy and friction compensation by NPID control are shown here for the first time. Construction of NPID control in state space is presented in section 2; extension of NPID control from regulator to tracking problems is presented in section 3; extension of NPID to systems with integral control is described in section 4, and friction compensation is addressed in section 5. Experimental results demonstrating tracking, improved tracking accuracy and friction compensation are presented in section 6; and the conclusions appear in section 7.

2 NPID control in state space

2.1 System model

Control of a linear, time-invariant, strictly proper state-space system is considered:

$$\dot{x}(t) = Ax(t) + Bu(t) \quad (4)$$
$$y(t) = Cx(t)$$

where $A \in R^{nxn}$, $B \in R^{nx1}$ and $C \in R^{1xn}$. Single-input, single-output systems are considered here. NPID control has been extended to MIMO systems, [15], but the integral control, tracking and friction compensation applications of the present paper are most naturally cast as SISO applications.

Control, $u(t)$, is given by the state feedback NPID control law:

$$u(t) = -K(x)\,x(t) + u_r(t) \quad (5)$$

$$K(x) = K_0 + s_{k_1}(x)\,k_1(x)\,K_1 + s_{k_2}(x)\,k_2(x)\,K_2 + \ldots \quad (6)$$

where $K(x) \in R^{1xn}$ is the time-varying state feedback gain; $K_0 \in R^{1xn}$ is the vector of feedback gains determining the low-gain controller; $K_1, K_2, \ldots \in R^{1xn}$ are feedback vectors of high-gain control; scalars $k_1(x), k_2(x), \ldots : R \to [0,\infty)$ are high-gain coefficients, they are nonnegative functions which determine the magnitude of the high-gain control; and $s_{k_1}(x), s_{k_2}(x), \ldots : R^n \to \{0,1\}$ are switch functions which determine when high-gain control may be applied; and the term $u_r(t)$ represents a possible reference input, and will be used in section 3 to facilitate tracking control. When $u_r(t) \equiv 0$ the system is a regulator, for which asymptotic stability is established by theorem 1 below; and when $u_r(t) \neq 0$ the system presents a tracking control problem, for which bounded-input bounded-output stability is established by theorem 2 below.

The dots in equation (6) indicate that there may be any number of high-gain terms $s_{k_i}(x)\,k_i(x)\,K_i$ in the expression for $K(x)$, though often there will be only one high-gain term.

Folding the control into the system matrix gives:

$$\dot{x}(t) = \hat{A}(x)\,x(t) + B u_r(t) \tag{7}$$

where

$$\begin{aligned} \hat{A}(x) &= A - BK(x) \\ &= A - BK_0 - s_{k_1}(x)\,k_1(x)\,BK_1 - \ldots \end{aligned} \tag{8}$$

is the closed-loop system matrix and is time varying on account of the time varying switch and high-gain coefficient functions $s_{k_i}(x)$ and $k_i(x)$.

The switch functions in control law (6) introduce discontinuity into the right hand side of differential equation (7). Relying on the treatment of variable structure systems developed by Paden and Sastry [17], it has been shown, [1], that differential equation (7) has a well defined solution when:

1. The switching functions exhibit finitely many discontinuities per finite volume of state space, and

2. The time-varying state feedback gain $K(x)$ is bounded above.

These conditions obtain for NPID control with bounded K_i and $k_i(t)$, and the switch function defined below.

For NPID control as described by equations (4-8), Lyapunov stability can be constructively established. Starting with a quadratic Lyapunov function

$$V(t) = x^T(t)\,P x(t) \tag{9}$$

where P is a constant, symmetric, positive definite matrix, the Lyapunov derivative is given by

$$\dot{V}(t) = x^T(t)\left(\hat{A}^T(x)P + P\hat{A}(x)\right)x(t) \tag{10}$$

During intervals when $s_{k_i}(\cdot) = 0$, the Lyapunov derivative is given by

$$\dot{V}(t) = x^T(t)\left(\widehat{A}_L^T P + P\widehat{A}_L\right)x(t) = -x^T(t)\,Q_L\,x(t) \tag{11}$$

where

$$\widehat{A}_L = A - BK_0 \tag{12}$$

and

$$-Q_L = \widehat{A}_L^T P + P\widehat{A}_L \tag{13}$$

When $s_{k_i}(\cdot) \neq 0$, $\dot{V}(t)$ may be written

$$\dot{V}(t) = -x^T(t)\,Q(x)\,x(t) \tag{14}$$

where

$$Q(x) = Q_L + s_{k_1}(x)\,k_1(x)\,Q_{k_1} + \ldots \tag{15}$$

and

$$Q_{k_i} = K_i^T B^T P + PBK_i \tag{16}$$

are *n*x*n* symmetric matrices.

Theorem 1. Asymptotic stability of NPID regulator control for state space systems (from [1])

Considering a linear, time-invariant, strictly-proper system, as given by Eqn (4), and NPID control, Eqn (6), with K_0 chosen to stabilize $\{A, B, C\}$, K_i bounded, and P chosen so that Q_L is positive definite; and choosing the switch functions so that

$$s_{k_i} = \begin{cases} 0 & (x^T Q_{k_i} x) < 0 \\ 0 \text{ or } 1 & (x^T Q_{k_i} x) \geq 0 \end{cases} \tag{17}$$

then the system with NPID control will be globally asymptotically stable for any bounded, nonnegative choice of $k_i(x)$.

Proof: Following the generalization of Lyapunov stability to discontinuous systems presented in [17, 18]; with $V(t)$ as given in Eqn (22) then, by choice of $s_{k_i}(x)$, Eqn (17), the second and subsequent terms in Eqn (15) make strictly non-positive contributions, and the Lyapunov derivative is upper bounded by:

$$\dot{V}^*(t) \leq -x^T Q_L x \equiv -w(x) < 0\,, \;\; ||x|| \neq 0 \tag{18}$$

which is assured to be negative definite by the stability of $\{A, B, C\}$ with controller K_0 .

2.2 Design of NPID control

Based on the stability result, the design of an NPID control proceeds by:

1. Determining the stabilizing low-gain controller, K_0, and forming $\widehat{A}_L$;
2. Selecting a Q_L matrix, and calculating P as the solution to the matrix Lyapunov Eqn (13);
3. Selecting the K_i, and determining Q_{k_i} from Eqn (16),
4. Selecting $k_i(x)$.

Thus the designer choices are K_i, which determines the direction in state space for high-gain control, and Q_L, which determines P. These together determine Q_{k_i}. Several design strategies have been proposed, including maximizing the volume of state space in which stiff control may be applied, [1]; design for control with partial state knowledge, [15, 19, 20]; and design for robustness, [21]. The selection of $k_i(\cdot)$ determines the magnitude of the nonlinear control effort.

3 Tracking NPID control

The details of a Lyapunov stability proof for the tracking case depend substantially on how the state feedback control is extended to tracking. One possibility is a feedforward term, which will bias the equilibrium output to be desired output: $u_r(t) = N_f\, y_d(t)$, where $u_r(t)$ is as defined in Eqn (5) and N_f is a scalar. Another possibility is control in error coordinates, which corresponds to $u_r(t) = K(x)\; x_d(t)$, but may be written:

$$u(t) = K(x)\; \tilde{x}(t) \tag{19}$$

where

$$\widetilde{x}(t) = x_d(t) - x(t) \tag{20}$$

and where $x_d(t)$ is the desired state and $\widetilde{x}(t)$ is the state error.

The construction of Eqns (19) and (20) is used here and relies on converting the state feedback to error coordinates. This construction has the advantage of being able to represent PID type control, but requires that the desired trajectory in each of the state variables be known. This requirement in turn places the restriction that the reference trajectory be sufficiently smooth for the necessary number of derivatives to exist, and that they are known. This condition is easily met in cases when the reference trajectory is generated by a path planner. In cases where the reference trajectory is based on sensed signals, the needed trajectories of the state variables can be generated by a reference model (e.g., [22]).

Applying control law (19), with $K(x)$ as given in Eqn (6); then the state derivative is given by:

$$\begin{aligned}\dot{x}(t) &= Ax(t) + BK(x)\,\widetilde{x}(t)\\ &= Ax_d(t) - (A - BK(x))\,\widetilde{x}(t)\\ &= Ax_d(t) - \widehat{A}(t)\,\widetilde{x}(t)\end{aligned} \tag{21}$$

where $\widehat{A}(t)$ is as given in Eqn (8). Writing the Lyapunov function

$$V(t) = \widetilde{x}^T(t)\; P\,\widetilde{x}(t) \tag{22}$$

gives the Lyapunov derivative:

$$\begin{aligned}\dot{V}(t) &= \dot{\widetilde{x}}(t)^T P\widetilde{x}(t) + \widetilde{x}^T(t)\,P\dot{\widetilde{x}}(t)\\ &= \widetilde{x}^T(t)\widehat{A}^T(t)\,P\widetilde{x}(t) + \widetilde{x}^T(t)\,P\widehat{A}(t)\widetilde{x}(t)\\ &\quad + \left(\dot{x}_d^T(t) - x_d^T(t)A^T\right) P\widetilde{x}(t)\\ &\quad + \widetilde{x}^T(t)\,P\,(\dot{x}_d(t) - Ax_d(t))\end{aligned} \tag{23}$$

Defining

$$\xi(t) = \dot{x}_d(t) - Ax_d(t) \tag{24}$$

the term $\xi(t)$ is the difference between the derivative of the desired state vector and that of the unforced system. Using (24) in (23) gives:

$$\dot{V}(t) = -\tilde{x}^T(t)\, Q(t)\, \tilde{x}(t) + 2\xi^T(t)\, P\tilde{x}(t) \tag{25}$$

where $Q(t)$ is as given in Eqn (15). The Lyapunov derivative (25) is used to establish BIBO stability for tracking control when $\xi(t)$ is bounded.

Theorem 2. Bounded Input – Bounded Output stability of NPID tracking control.

Considering a linear, time-invariant, SISO, strictly-proper system, as given by Eqn (4); and NPID control, Eqn (19), with K_0 chosen to stabilize $\{A, B, C\}$, K_i bounded, and a reference trajectory with $x_d(t)$ and $\dot{x}_d(t)$ such that $\xi(t)$ of Eqn (24) is bounded: $||\xi(t)|| < \overline{\xi}$; and P chosen so that Q_L is positive definite; and choosing the switch functions so that

$$s_{k_i} = \begin{cases} 0 & (x^T Q_{k_i} x) < 0 \\ 0 \text{ or } 1 & (x^T Q_{k_i} x) \geq 0 \end{cases} \tag{26}$$

then the system with NPID control will show bounded input - bounded output stability for any bounded choice of $k_i(x) \geq 0$.

Proof: because the term $-\tilde{x}^T(t)\, Q(t)\, \tilde{x}(t)$ in Eqn (25) is both strictly negative and quadratic in $\tilde{x}(t)$, and because the term $2\xi^T(t)\, P\tilde{x}(t)$ is bounded and linear in $\tilde{x}(t)$; for any $\overline{\xi}$ there exists a finite $\overline{\tilde{x}} \in R^+$ sufficiently large to ensure that for all $\left\{\tilde{x}(t) : ||\tilde{x}(t)|| > \overline{\tilde{x}}\right\}$, we have $\dot{V}(t) < 0$.

Qualitatively, the quadratic term in Eqn (25) may be relied upon to dominate the linear term. A sharp bound $\overline{\tilde{x}}$ may be difficult to determine, but a sufficient bound is given by:

$$\overline{\tilde{x}} \geq 2\frac{|\lambda(P)|_{\max}}{|\lambda(Q)|_{\min}}\overline{\xi} \tag{27}$$

where $|\lambda(\cdot)|_{\max}$ refers to the largest eigenvalue of P and $|\lambda(Q)|_{\min}$ refers to the the smallest eigenvalue of Q.

4 Augmented state vector: integral control

In many cases it is desirable to apply integral error feedback (integral control). NPID control can be extended to systems with integral control by augmenting the state vector with controller states, as illustrated in Eqn (28).

$$\begin{aligned} \dot{x}_a(t) &= A_a x_a(t) + B_a u(t) \\ y(t) &= C_a x_a(t) \end{aligned} \tag{28}$$

where

$$A_a = \begin{bmatrix} A & \vdots & A_{pc} \\ \cdots & \cdots & \cdots \\ A_{cp} & \vdots & A_{cc} \end{bmatrix}$$

is the augmented system matrix;

and where	$x_a(t) = \left[x^T, x_c^T\right]^T$	is the augmented state vector;
	$x_c(t)$	is the vector of added controller states;
	A_{pc}, A_{cp}	are coupling terms, the dependence of controller stateson system states will appear in A_{cp};
	A_{cc}	reflects the dynamics of the controller states;
	$B_a = \left[B^T, B_c^T\right]^T$	is the augmented input vector;
	$C_a = [C, \phi]$	is the augmented output vector, ϕ is the zero vector;
and where		$A_{pc}, A_{cp}, A_{cc}, B_c$ and ϕ are appropriate size.

Choosing $A_{cp} = C$, with $A_{cc} = \phi$ and $B_c = \phi$ gives $x_c(t) = \int y(\tau)\,\mathrm{d}\tau$ and the corresponding element of the augmented K vector gives integral feedback.

Starting with the augmented system, (28), the development of theorem 1 carries through directly; establishing for the regulator case that the integral of the output goes to zero (when no disturbance is present). For the tracking case, the possibility exists that controller states in $x(t)$ and $x_d(t)$ may grow without bound[1]. In the usual case that the open-loop plant states do not depend on

[1]For example, with a set point of $y_d(t) = 1$, $\int y(t)\,\mathrm{d}t$ and $\int y_d(t)\,\mathrm{d}t$ grow indefinitely; but if the system is stable, $\int e(t)\,\mathrm{d}t = \int y_d(t)\,\mathrm{d}t - \int y(t)\,\mathrm{d}t$ will be bounded.

the controller states, i.e., $A_{pc} = \phi$, and the plant input does not affect the controller state derivative, i.e., $B_c = 0$, then the controller states and their derivative cancel in Eqn (24). Hence, even though the integral term contained in $x(t)$ and $x_d(t)$ can grow continuously, $\xi(t)$ does not, and theorem 2 establishes that $\widetilde{x}(t)$ is bounded.

When the state space system is in observable canonical form the output and its derivatives comprise the state vector, and state feedback can directly represent PD or PID control. Because there is no requirement that all of the elements of $K(x)$ be non-zero, this is true even for higher-order systems. And conversely, if the non-zero elements of K_0 and K_i correspond to the proportional, integral or derivative terms; NPID control designed in state space can be implemented as a series PID controller; as was done for the experimental demonstrations of section 6. The results of theorems 1 and 2 carry over directly to this implementation; only evaluation of s_{k_i} requires knowledge of the full state vector.

Comparison of the present state feedback results with past results cast in Proportional-Derivative form, [1, 11, 19, 21], shows that consideration of state feedback simplifies the analysis while at the same time offers greater design freedom and removes a previously necessary restriction on the sign of the product (CB).

5 Friction compensation

Increasing system stiffness is a common method of friction compensation, in part because it does not require an accurate friction model [23]. With C chosen so that $y(t)$ is the position output of the system, and $e(t)$ is the position error, then for NPID control to compensate static friction, states $\{\widetilde{x}(t) : \dot{y}(t) = 0, e(t) \neq 0\}$ must be included in the region where high-gain is allowed: $\left(\widetilde{x}^T Q_{k_i} \widetilde{x}\right) > 0$.

Choosing $K_i = C$ so that the i^{th} high-gain term will compensate output error, and by breaking the state vector into components parallel and perpendicular to the output, it is possible to determine whether static friction will be compensated. Writing:

$$\widetilde{x}_e(t) = C^T \frac{C\,\widetilde{x}(t)}{CC^T} \quad \text{and} \quad \widetilde{x}_\perp(t) = \widetilde{x}(t) - \widetilde{x}_e(t) \tag{29}$$

where $\widetilde{x}_e(t)$ is the portion of $\widetilde{x}(t)$ determining $e(t)$, and $\widetilde{x}_\perp(t)$ lies in the remaining $(n-1)$ dimensions of state space; then the switch function term $\left(\widetilde{x}^T Q_{k_i} \widetilde{x}\right)$ can be broken into 3 components:

$$
\begin{aligned}
\left(\widetilde{x}^T Q_{k_i}\widetilde{x}\right) &= \left(\widetilde{x}_e^T Q_{k_i}\widetilde{x}_e\right) + \left(\widetilde{x}_\perp^T Q_{k_i}\widetilde{x}_\perp\right) + 2\left(\widetilde{x}_e^T Q_{k_i}\widetilde{x}_\perp\right) \\
&= \left(\frac{C\widetilde{x}}{CC^T}\right)^2 \left(CC^T\right)\left(B^T PC^T + CPB\right) \\
&\quad + \left(\widetilde{x}_\perp^T Q_{k_i}\widetilde{x}_\perp\right) + 2\left(\widetilde{x}_e^T Q_{k_i}\widetilde{x}_\perp\right)
\end{aligned} \tag{30}
$$

Proposition 3. Friction compensation by NPID control.

Given the system as describe for theorem 1 or theorem 2 above, if

$$CPB > 0 \tag{31}$$

then $\widetilde{x}^T Q_{k_i}\widetilde{x} > 0$ for $e(t) \neq 0$ and $\widetilde{x}_\perp(t)$ sufficiently small.

Proof: Given condition (31) and $e(t) \neq 0$, the first term in Eqn (30) will be strictly positive. With $\widetilde{x}_\perp(t)$ sufficiently small the first term will dominate, giving $\left(\widetilde{x}^T Q_{k_i}\widetilde{x}\right) > 0$ and enabling high gain for friction compensation.

Proposition 3 provides a direct test for when NPID control will compensate static friction. When $CPB > 0$, NPID control will compensate static friction for states $\{\widetilde{x}(t) : \dot{y}(t) = 0, e(t) \neq 0\}$ when acceleration and other state variables are not too large. Note that for the tracking case, the velocity term of $\widetilde{x}(t)$ includes the desired velocity, and so may be non-zero, even when $\dot{y}(t) = 0$. The restriction that $\widetilde{x}_\perp(t)$ be small is not a practical problem, since the influence of static friction is greatest when desired velocities and accelerations are small. Friction compensation is demonstrated with the implementation of the next section.

6 Experimental results

NPID control has been implemented for the SRV-02B motor servo from Quanser Consulting. The motor servo is seen in figure 2, with a schematic provided in figure 3, and principle parameters listed in table 1. The MicroMo motor is equipped with an integral tachometer and the output position is sensed with a potentiometer. Parameter identification via frequency response gives the transfer function model:

$$\frac{\theta(s)}{V(s)} = \frac{b_0}{s(s/a_0+1)} \tag{32}$$

which gives the state space model (constructed for integral control and tracking):

$$\begin{gathered} x(t) = \begin{bmatrix} \dot{y}(t) & y(t) & \int y(t)\,\mathrm{d}t \end{bmatrix}^T \\ A = \begin{bmatrix} -2.36 & 0 & 0 \\ 1 & 0 & 0 \\ 0 & 1 & 0 \end{bmatrix} \quad B = \begin{bmatrix} 13.90 \\ 0 \\ 0 \end{bmatrix} \quad C = \begin{bmatrix} 0 & 1 & 0 \end{bmatrix} \end{gathered} \tag{33}$$

The control law used is given by Eqns (19) and (20), with $K(x)$ given by Eqn (6). The low gain control was chosen to be the PID controller: $K_0 = \begin{bmatrix} 2.778 & 33.33 & 100 \end{bmatrix}$ which gives closed-loop poles at: $s = \begin{Bmatrix} -24.2 & -12.0 & -4.8 \end{Bmatrix}$. This is a stiff linear control for this system and was designed by the root locus method with the compensator zeros were set at $s = -6.0$ [sec^{-1}]. This low-gain controller was chosen as a stiff and well damped control which remains within the actuator limits over the range of test motions.

Parameter	Value (Mechanical Parameters Reflected to Output)
Motor Description	MicroMo Electronics Model 2842S006 C001G
Torque Constant	0.1537 [N-m/Amp]
Resistance	7.2 Ohms Total (Motor + Series Resistor)
Inductance	0.145 mH
Motor and Load Inertia	0.000775 [Kg-m^2]
Coulomb Friction	0.015 [N-m]
Position Sensor Sensitivity	0.6044 $\pm$ 0.002 [rad/volt]
Gear Ratio	14:1
Tachometer Sensitivity	7.48 $\pm$ 0.01 [rad/sec/volt]
Rated Average Power	0.05 HP
Transfer Function Parameters	
a_0	2.36 $\pm$0.15 [s-1]
b_0	5.89 $\pm$ 0.3 [rad/volt-s]

Table 1: Parameters of the SRV-02B Motor Servo. Uncertainties reflect 90% confidence range.

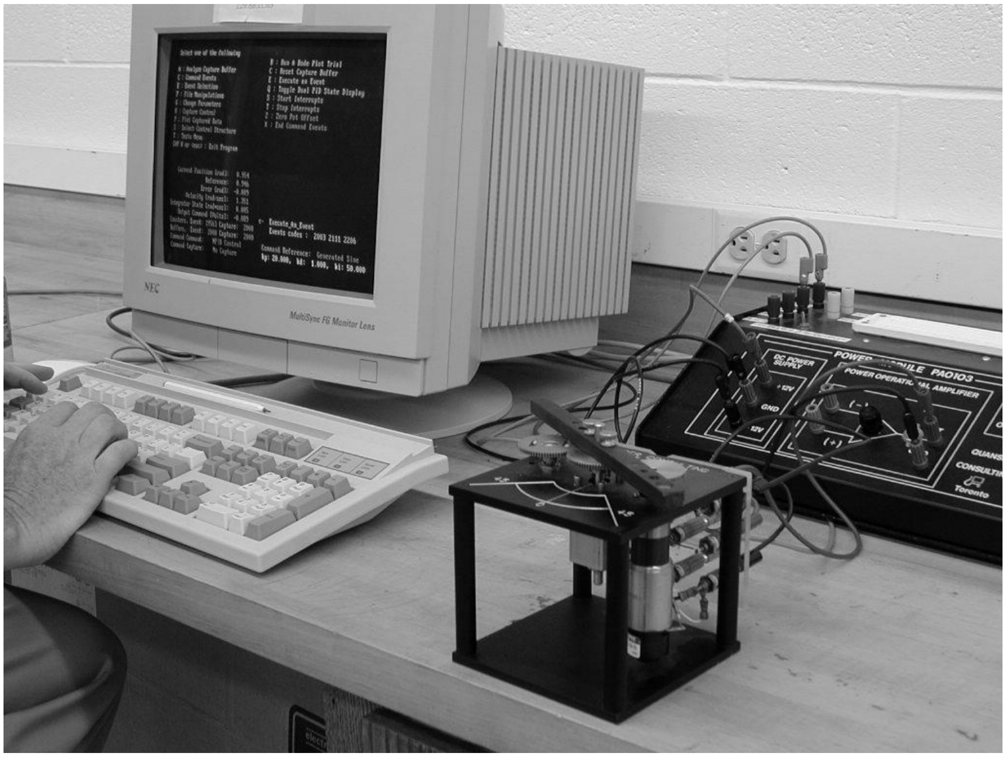

Figure 2: SRV-02B Motor Servo.

Choosing Q_L to be the identity matrix and $K_1 = \begin{bmatrix} 0 & 33.33 & 0 \end{bmatrix}$ gives:

$$Q_{k_1} = \begin{bmatrix} 0 & 0.1582 & 0 \\ 0.1582 & 0.9750 & 0.004201 \\ 0 & 0.004201 & 0 \end{bmatrix} \tag{34}$$

where Q_{k_1} has been scaled to have a norm of 1. This choice for K_1 increases the stiffness of the system to position error. The second element of K_0 is k_p of the PID control (cf. Eqn (1)). Taking this value, 33.33 [volts/radian], to be the corresponding element of K_1 gives the high-gain coefficient $k_1(x)$ the sense of being a factor multiplying the low gain control. Thus, if $k_1(x)$ takes a maximum value of 5.0, the NPID control has a maximum of 6 times the stiffness of the low-gain control.

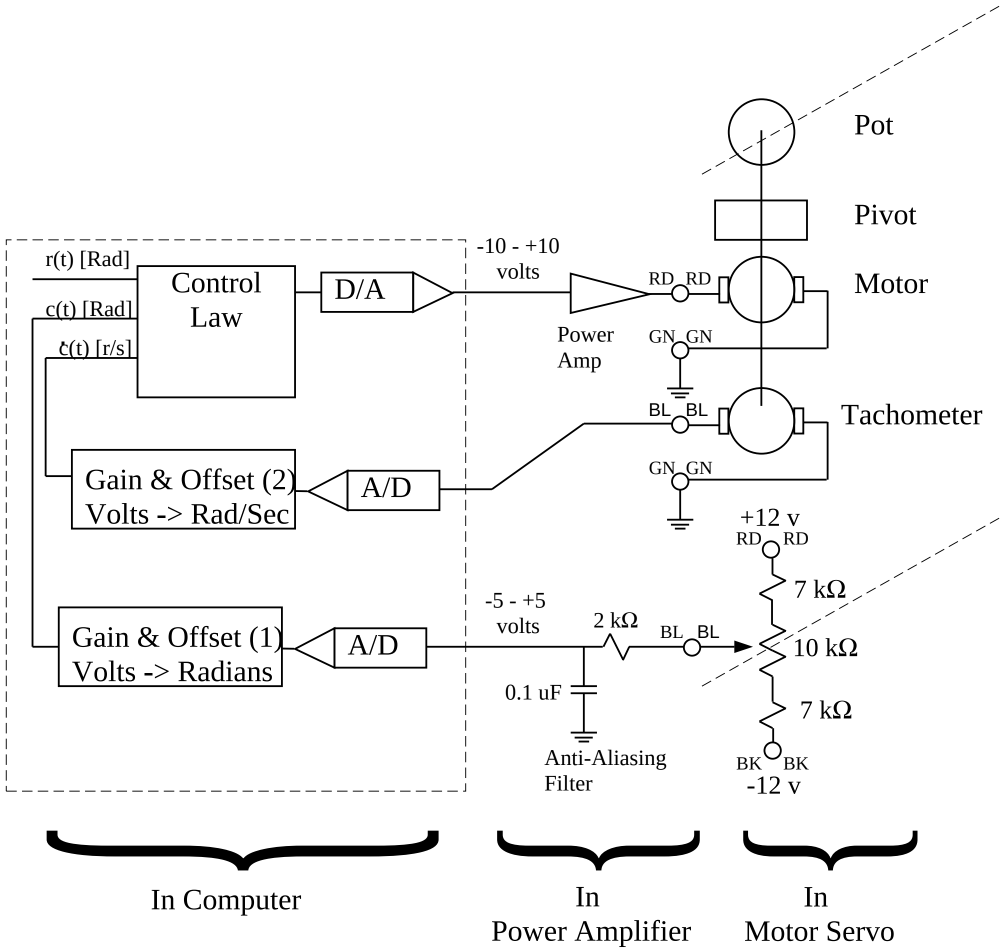

Figure 3: Schematic diagram of the SRV-02B motor servo.

6.1 Implementation Issues

To smooth the transition from low to high gain, the high-gain coefficient was implemented with:

$$k_1(\tilde{x}) = m_1 \frac{q_1(\tilde{x})}{q_1(\tilde{x}) + q_0}$$
$$q_1(\tilde{x}) = \frac{\tilde{x}^T Q_{k_1} \tilde{x}}{\sqrt{\tilde{x}^T \tilde{x}}} \tag{35}$$

where m_1 is the maximum value taken by $k_1(\tilde{x})$ [15, 16]. Function $k_1(\tilde{x})$ given by Eqn (35) assures that the transition from low- to high-gain control is not discontinuous, and reduces chatter. Parameter q_0 determines the width of the region over which the transition occurs, and was tuned to

$q_0 = 0.006$ as a compromise between reduced chatter (large q_0) and greatest effect of NPID control (small q_0). Additionally, $q_1(\tilde{x})$ was low-pass filtered to eliminate rapidly varying control arising with sensor quantization noise.

Motion, error and control variables for sinusoid tracking with PID and NPID control are shown in figure 4. The maximum high-gain coefficient of NPID control, m_1, is 5.0 for the trial of figure 4, corresponding to a proportional term increased from 33.33 to 200 [volts/radian]. The control effort seen in figure 4 shows chatter. Subsequent to these experiments, Kusik has investigated chatter [16] and found that it arises with non-ideal attributes of the system: sensor quantization and other noise and sampling delay. By optimizing sensor characteristics and sample rate, and modifying the behavior of NPID control around zero error, Kusik found that chatter could be reduced by 75%.

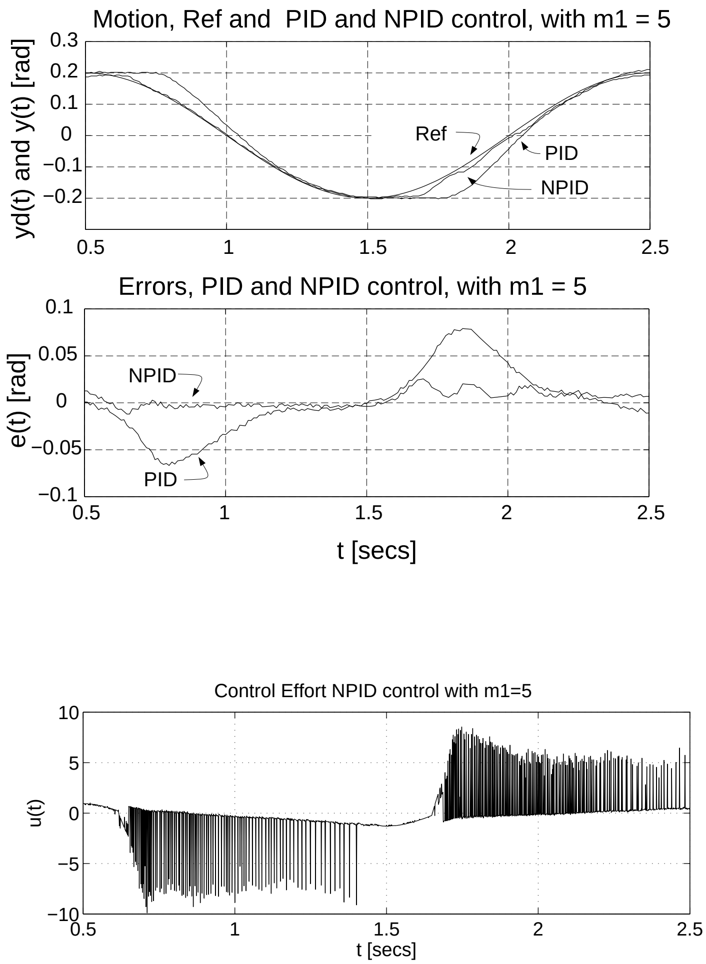

Figure 4: Motion error and control for PID and NPID control.

Figure 5 shows that RMS tracking error steadily decreases with increasing high gain, with

$m_1 = 5.0$ giving as much as a 15 dB reduction of tracking error. In the middle frequency range, reduction of tracking error is approximately proportional to the increase in k_p. Note that $m_1 = 0.0$ in figures 5-7 corresponds to linear PID control.

It might be expected that NPID control would result in increased control action; but figures 6 and 7 show that this is not the case. The RMS command corresponding to the motions of figure 5 is reported in figure 6. Up to 10.0 [rad/sec] the RMS commands are very tightly grouped, and indeed, in the range 1.0 to 2.0 [rad/sec] the NPID command levels with $m_1 = 1.0$ are *lower* than the corresponding PID command levels. We believe that the reduction of control effort arises with the interaction of integral control and friction, and the friction compensation provided by NPID control.

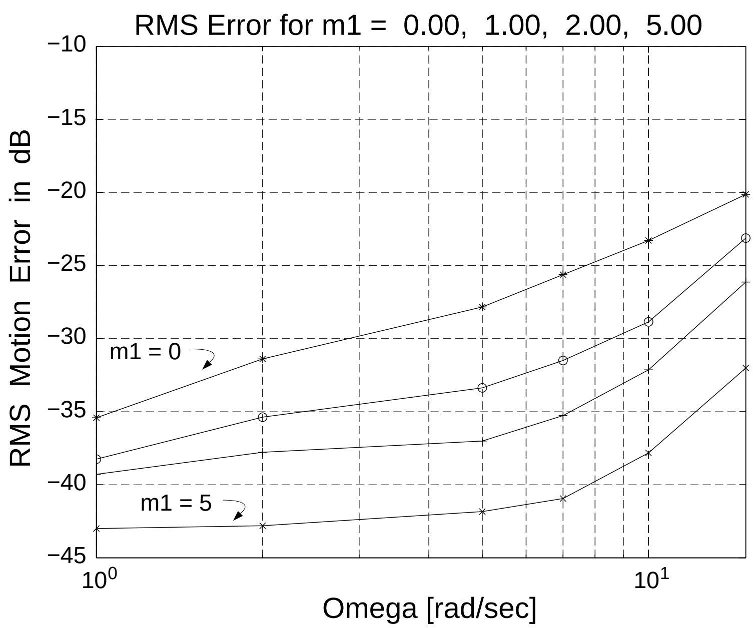

Figure 5: RMS tracking error for sinusoids between 1.0 and 15.0 [rad/sec], amplitude = 0.2 [rad], and $m_1 = 0{,}0,\ 1.0,\ 2.0 \mathrm{and} 5.0$.

The peak command levels are plotted in figure 7. The experimental hardware saturates at 10 [volts]. Again it is seen that doubling or tripling the proportional gain ($m_1 = 1.0$ or 2.0) results in very little increase of the peak command, and possibly a reduction. Choosing $m_1 = 5.0$ approximately doubles the peak control action at low frequencies.

For the experimental system and the NPID switching function described by Eqn (34), the sectors on which high gain can be applied are seen in figure 8. The state space of the system is 3 dimensional, and so figure 8 is a 2-D slice taken at $\int y(t)\, \mathrm{d}t = 0$. The figure shows that stiff control can be applied on a large subset of state space. The I and III quadrants correspond to heuristically motivated case for NPID control: conditions in which the error is increasing. The straight line bisecting the II and IV quadrants is a natural consequence of the test $\left(\widetilde{x}^T Q_{k_1} \widetilde{x}\right) > 0$, but has the interesting interpretation of a time to arrive at $e(t) = 0$. In the case of figure 8, if the time to arrive at $e(t) = 0$ is greater than 0.324 seconds, stiff gain is allowed.

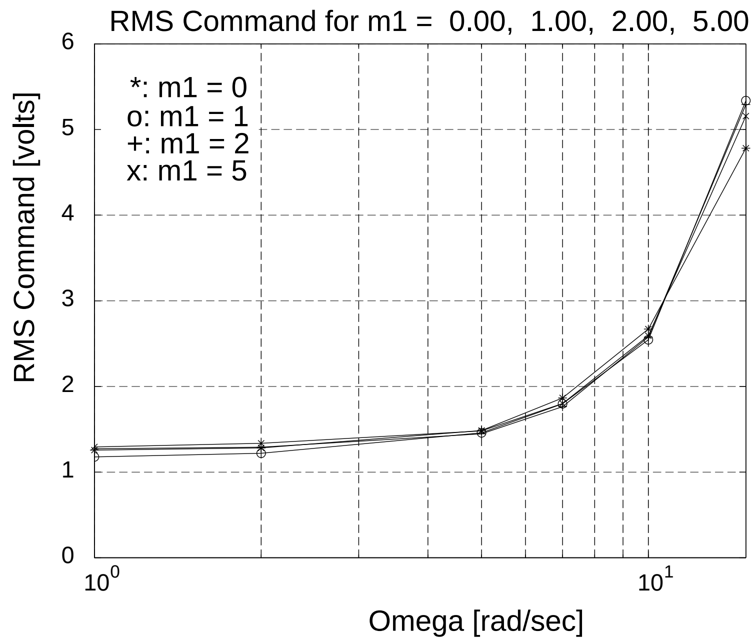

Figure 6: RMS command in [volts] for $m_1 = 0,0,\ 1.0,\ 2.0\,\text{and}\,5.0.$

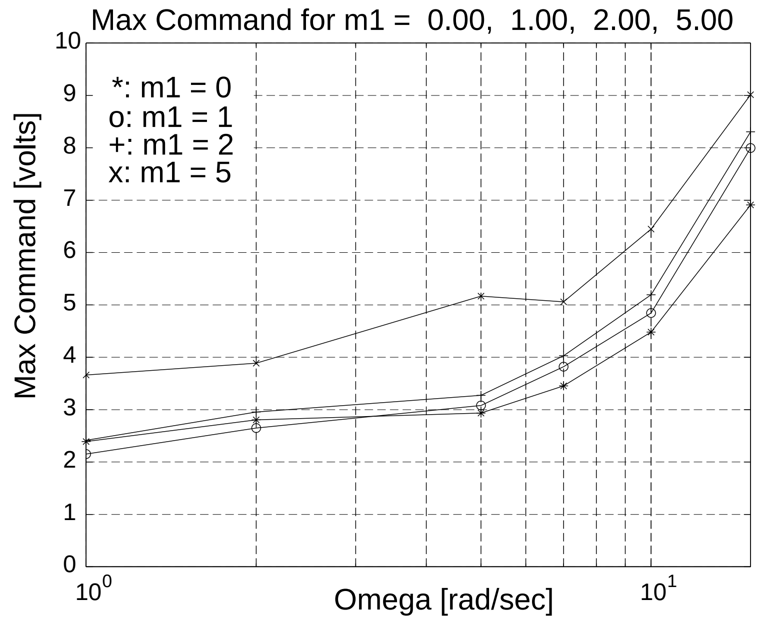

Figure 7: Maximum command in [volts] for $m_1 = 0, 0,\ 1.0,\ 2.0$ and 5.0.

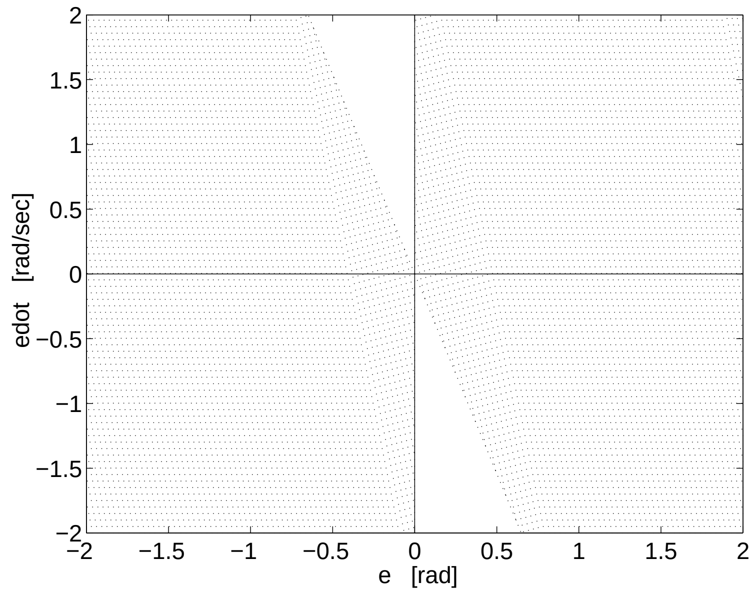

Figure 8: Sectors on which high gains are enabled; a 2-D cross section of the 3-D state space taken at $\int e(t)\, \mathrm{d}t = 0$.

6.2 Friction Compensation

Applying the test of proposition 3 gives $CPB = 0.5658 > 0$, establishing that high-gain control can be applied when there is stiction. This is also seen in figure 8, where it is seen that when $e(t) \neq 0$, high-gain control is allowed for a large range of $\dot{e}$, including $\dot{e} = 0$.

Figure 5 shows improved tracking accuracy with NPID control. But because NPID control reduces tracking error even when friction is not present, it is difficult to separate the impact of friction compensation from the general impact of NPID control. One way to assess friction compensation is to measure the residual in the motion error signal, after the sinusoidal component at the frequency of the reference signal has been removed. Friction, being the dominant, error-inducing nonlinearity will make the dominant contribution to this residual error. The residuals, for several values of m_1 are listed in table 2, which shows that the residual error is reduced by increasing the NPID control.

Maximum High-Gain Coefficient, m_1	Motion Error Residual [rad]
0	0.0154
1	0.0116
2	0.0081
5	0.0069

Table 2: Motion error residual for several values of m_1.

7 Conclusions

The art of NPID control has been advanced in several directions. The known stability results have been extended to state feedback, tracking and integral control. NPID control had previously been applied to improve the damping of lightly damped systems; but the present results show that increased tracking accuracy is also possible, and that NPID control can improve compensation for friction.

The investigation of NPID control continues to raise more questions than it answers. For example, the design guidelines presented thus far are based solely on stability, and no methodology exists to design to performance goals; or sliding modes have been detected in NPID controllers and systems with friction, and the properties of these sliding modes remain to be explored. These and other questions are the objects of ongoing work.

References

[1] B. Armstrong, J. McPherson, and Y. Li, "Stability of Nonlinear PD control," *Applied Mathematics and Computer Science*, vol. 7, no. 2, pp. 101–120, 1997. Invited Paper.

[2] S. C. Jacobsen, J. E. Wood, D. F. Knutti, and K. B. Biggers, "The Utah/MIT dextrous hand: work in progress," *Inter. Journal of Robotics Research*, vol. 3, no. 4, pp. 21–50, 1984.

[3] N. J. Krikelis, "State feedback integral control with 'intelligent' integrators," *Inter. J. of Control*, vol. 32, no. 3, pp. 465–473, 1980.

[4] R. M. Phelan, *Automatic Control Systems*. Ithaca: Cornell University Press, 1977.

[5] W. J. Rugh, "Design of nonlinear PID controllers," *AIChE Journal*, vol. 33, no. 10, pp. 1738–1742, 1987.

[6] S. M. Shahruz and A. L. Schwartz, "Design and optimal tuning of nonlinear I compensators," *J. of Optimization Theory and Applications*, vol. 83, no. 1, pp. 181–98, 1994.

[7] S. M. Shahruz and A. L. Schwartz, "Nonlinear PI compensators that achieve high performance," *J. of Dynamic Systems, Measurement and Control*, vol. 119, pp. 105–110, Oct 1997.

[8] J. Taylor and K. Strobel, "Nonlinear compensator systhesis via sinusoidal-input describing functions," in *Proc. American Control Conf.*, pp. 1242–47, Boston: AACC, 1985.

[9] H. Seraji, "A new class of nonlinear PID controllers with robotic applications," *J. Robotic Systems*, vol. 15, no. 3, pp. 161–181, 1998.

[10] J. H. Taylor and K. J. Åström, "Nonlinear PID autotuning algorithm," in *Proceedings of the 1986 American Control Conference*, pp. 2118–2123, Seattle: AACC, 1986.

[11] Y. Xu, J. M. Hollerbach, and D. Ma, "A nonlinear PD controller for force and contact transient control," *IEEE Control Systems Magazine*, vol. 15, no. 1, pp. 15–21, 1995.

[12] B. Armstrong, D. Neevel, and T. Kusik, "New results in NPID control: Tracking, integral control, friction compensation and experimental results," in *Proc. of the 1999 Inter. Conf. on Robotics and Automation*, pp. 837–842, Detroit: IEEE, 1999.

[13] H. Seraji, "Nonlinear and adaptive control of force and compliance in manipulators," *Inter. J. of Robotics Research*, vol. 17, no. 5, pp. 467–484, 1998.

[14] Y. Xu, J. M. Hollerbach, and D. Ma, "Force and contact transient control using nonlinear PD control," in *Proc. of the 1994 Inter. Conf. on Robotics and Automation*, pp. 924–930, Atlanta: IEEE, 1994.

[15] B. Armstrong and B. Wade, "Nonlinear PID control with partial state knowledge: damping without derivatives," *Inter. Journal of Robotics Research*, vol. 19, no. 8, pp. 715–731, 2000.

[16] T. P. Kusik, "Chatter in nonlinear proportional-integral-derivative (npid) control, causes and remedies," Master's thesis, University of Wisconsin – Milwaukee, 1999.

[17] B. E. Paden and S. S. Sastry, "A calculus for computing Filippov's differential inclusion with application to the variable structure control of robot manipulators," *IEEE Trans. on Circuits and Systems*, vol. CAS-34, no. 1, pp. 73–82, 1987.

[18] A. F. Filippov, *Diffenential Equations with Discontinuous Righthand Sides*. Dordrecht, The Netherlands: Kluwer Academic Publishers, 1988.

[19] B. Armstrong, "Nonlinear PD control with incomplete state knowledge: damping without derivatives," in *Proc. of SYROCO '97*, pp. 73 – 78, IFAC: Nantes, France, 1997.

[20] B. Armstrong and B. A. Wade, "Nonlinear PID control with partial state knowledge: A general method based on quadratic programming," in *Proc. 2000 American Controls Conference*, pp. 774–778, AACC: Chicago, 2000.

[21] B. Armstrong, "Robustness of NPD control (preliminary results)," in *Proc. of IROS '97*, pp. 478–483, IEEE: Grenoble, France, 1997.

[22] J.-J. E. Slotine and W. Li, *Applied Nonlinear Control*. Englewood Cliffs: Prentice Hall, Inc., 1991.

[23] B. Armstrong, P. Dupont, and C. C. de Wit, "A survey of models, analysis tools and compensation methods for the control of machines with friction," *Automatica*, vol. 30, no. 7, pp. 1083–1138, 1994.